RASĀYAN *J. Chem.*
Vol. 16 | No. 1 |268-275| January - March | 2023
ISSN: 0974-1496 | e-ISSN: 0976-0083 | CODEN: RJCABP
http://www.rasayanjournal.com
http://www.rasayanjournal.co.in

MICROWAVE IRRADIATION SYNTHESIS OF NITROGEN-DOPED Ag/MWCNT/ZnO NANOCOMPOSITE FOR PHOTOCATALYTIC APPLICATION

M. Singh[1], P. Kumar[2], N. S. Singh[3] and A. Jain[1,✉]
[1]Department of Electronics, Rajdhani College, University of Delhi, Delhi-110015, India
[2]Department of Chemistry, Rajdhani College, University of Delhi, Delhi-110015, India
[3]Department of Physics, Hindu College, University of Delhi, Delhi-110007, India
✉Corresponding Author: amit.jain@rajdhani.du.ac.in

ABSTRACT

In this proposed research work, Zinc oxide is fabricated with carbon nanotubes, nitrogen, and silver. The conclusion of the distinctive hybrid of dopants on the ZnO/MWCNT nanocomposite was studied. Acidic and basic nature dyes are used to check the efficiency of the composite photocatalyst. The hydrothermal & microwave route was adapted for combining mesoporous nanocomposite samples. The XRD analysis confirmed the information to the nanoscale crystal with the hexagonal dimension of ZnO. The observation of UV-vis spectra validates its photocatalytic competency in the visible beam as an outcome of the reduction in the bandgap energy. The proficiency of the photocatalyst was additionally entrenched over the axing in electron-hole recombination activity referring to dwindling PL intensity. The BET inspection supports the mesoporous structures of the samples. The SEM micrograph revealed the existence of agglomeration in nanoparticles with MWCNT while the perusal of TEM images established the existence of a 16–24 nm diameter of the MWCNT. Furthermore, the EDX analysis confirmed the presence of the Zn, N, O, Ag, and C.

Keywords: Hydrothermal, Microwave Irradiation, MWCNT, Silver, Nitrogen, Zinc oxide, and Photocatalysis.
RASĀYAN *J. Chem.*, Vol. 16, No.1, 2023

INTRODUCTION

The visible-light responsive photocatalytic ZnO nanostructures have been synthesized by two approaches, i.e., co-doping and nanocomposite formation. The doping of ZnO with another metal oxide (i.e., Ag) has been reported in several works.[1,2] The ZnO-coupled with silver exhibits numerous advantages such as the generation of electrons/holes.[3] The availability of clean and affordable water has become one of the prime challenges in the 21st century.[4] The freshwater available on earth is only 3% which is further distributed unevenly in various parts of the globe in the form of freshwater lakes, rivers, streams, glaciers, and underground aquifers.[5] Unfortunately, anthropogenic activities have polluted these sources of water leading to water scarcity across the world.[6–9]

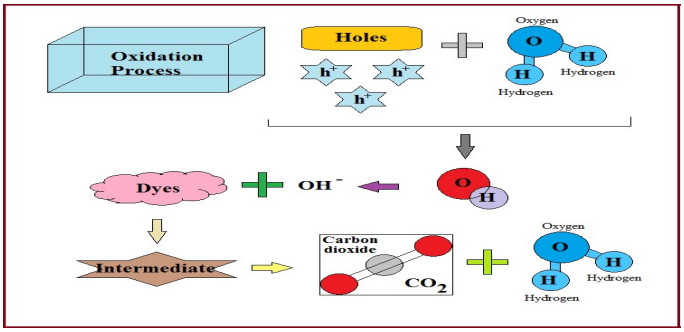

Fig.-1: The General Scheme of the Photocatalytic Process

Several approaches to impurity removal include; adsorption, chemical precipitation, sedimentation, and various biological ways. However, these techniques generally cause the generation of secondary pollutants.[10] Photocatalysis has presented a strong candidate among wastewater treatment technologies owing to its prodigious potential and high efficiency.[11] It can also employ sunlight to get rid of organic

http://doi.org/10.31788/RJC.2023.1618076

pollutants and harmful microbes by using solid photocatalysts (Fig.-1).[12] A perfect catalyst must be activated by the photons of visible light, chemically stable, and non-reactive.[13] SnO_2, TiO_2, CdO, ZnO, and their composites are acceptable photocatalysts to eliminate unrefined water.[14–16] The bandgap of these semiconductors allows absorption in the only UV region (388 nm) which corresponds to only 4% of the solar radiation. Thus, the visible region (400 to 700 nm) that constitutes 40% of the solar spectrum remains unused in such cases. Also, the TiO_2 and ZnO exhibit a maximum e^--h^+ recombination speed which affects the degradation rate of pollutants.[17] All these drawbacks limit the photo-degradation potency of the photocatalyst. A simple method to increase the separation of the charge carried by doping of transition element in the semiconductor is to consider and grow the energy limit of photoexcitation.[18] Doping of metals particularly Ag, Cu, Fe, Mn, Cr, Au, Ce, Sm, and non-metals like N, S, B, F, and C play a critical function to dwindle the band gap energy inclusive of charge carrier recombination rate.[19,20] The concept of mesoporosity arises to provide maximum surface area per gram of sample, so that maximum photocatalysis can be achieved from less quantity of photocatalyst sample.[21] Saleh *et al.* prepared MWCNT/ZnO embedded nanocomposite for acetaldehyde removal.[22] CNT/ZnO nanocomposite prepared by Ahmad *et al.* for photodegradation of Rhodamine B.[23] The hydrothermal method used by Liu *et al.* for ZnO/MWCNT nanocomposite.[24] ZnO/Al/CNT nanocomposite doped with ZnO has been prepared by Bu *et al.* via the sol-gel method.[25] The drop coating method has been used by Elias *et al.* for $Zn_3(PO_4)_2$/CNT nanocomposite.[26] ZnO/TiO_2/CNT has been fabricated by Dalt *et al.* for photocatalysis.[27] Reddy *et al.* fabricated ZnO/CNT nanocomposite for photocatalysis.[28] Jing *et al.* prepared ZnO/CNT nanocomposite for photocatalytic application.[29] ZnO/MWCNT nanocomposite fabricated by Saleh *et al*.[30] ZnO/CNT nanocomposite doped with nitrogen has been prepared by Elias *et al.* for photodegradation application.[31] Okeil *et al.* prepare ZnS/ZnO@CNT and ZnS@CNT for photocatalysis.[32] Cadmium doped ZnO/CNT has been prepared through the microwave method by Azqhandi *et al.*[33] MWCNT/ZnO nanocomposite doped with nitrogen and iron has been prepared by N. Chauhan *et al.* via a hydrothermal approach.[34] M. Basit *et al.* fabricate ZnO/CNT nanocomposite by vapor-liquid-solid process.[35] L.M. Cursaru *et al.* prepared ZnO-CNT nanocomposite in a high-pressure state.[36]

EXPERIMENTAL

The Chemical Utilized

The chemical employed in the experimental work belongs to Sigma Aldrich. De-ionized water, Sodium hydroxide pellets, Urea, Zinc Chloride, Silver nitrate, Methylene blue, and Congo red dyes are used.

Synthesis of ZnO/MWCNT Nanocomposite

As shown in Fig.-2, Solution 1 contains 0.1 gram of MWCNT in 25 ml of water and 1 molar concentration of zinc chloride (subjected to 1-hour sonication). Solution 2 contains 1 molar solution of sodium hydroxide added dropwise to solution 1 so that a white precipitate is obtained after microwave treatment (solution 3). Hydrothermal treatment at 180 degrees Celsius for 24 hours is provided for solution 3. The white powder has been obtained after filtration, washing, and drying.[34] Table-1 shows the chemical compositions of the samples. MWCNT has been prepared by the CVD process as mentioned in Escobar M. *et al.*[37]

RESULTS AND DISCUSSION

Study of Photocatalytic Degradation of Dyes

This process is employed to measure the photocatalytic capability of organized catalysts against target dyes. In this process, the aqueous solution dye is to be checked i.e., the target dye is subjected to artificial light (430-530 nm) in the presence of prepared photocatalysts (0.1 gm in 200 ml dye solution). Before exposure to light, the prepared suspension is treated under sonication for 30 minutes in dark. Briefly, the dye solution is brought in close vicinity of a light source that is irradiated from the top of the target sample. The target solutions generally get decolorated during this process. During this process, the concentration/intensity of the color and degradation rate are monitored (adsorption is checked) at rapid intervals (15 minutes) through UV-Vis spectroscopy, whereas the same solution without the photocatalyst act as a reference.[38]

X-Ray Diffraction

The X-ray diffractometer (PANalytical) excites the sample to delocalize the inner-shell electrons of the sample material leading to characteristic X-Ray production. In Fig.-4, X-ray diffraction spectra reveal wurtzite, highly crystalline, and hexagonal structure of ZnO (JCPDS No: - 800075) with its corresponding

miller indices. Two extra peaks in samples P_2, P_3, and P_4 at 38.09° and 44.30°, belong to silver (JCPDS No:- 841261). Peaks at 31.71°, 34.33°, 36.18°, 47.45°, 56.51°, 62.81°, 67.90°, and 69.02°refers to the wurtzite ZnO crystal.[39] The crystal size, as determined by using Debye- Scherrer formula ($D = 0.94\lambda/\beta\cos\theta$) increases with an increase in doping percentage i.e., 18.17, 19.12, 21.07, and 23.22 nm for P_1, P_2, P_3, and P_4.

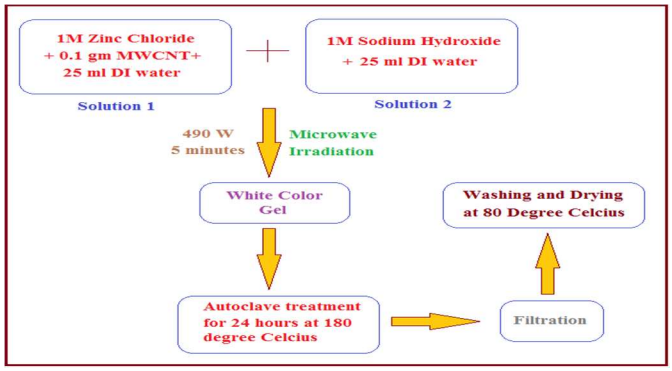

Fig.-2: The General Scheme of the Experimental Process

Table-1: Elements of Composition with Sample Code

S. No.	1	2	3	4
Chemical composition	0.1 g MWCNT + ZnO	MWCNT (0.1 g) + Silver (2%) + ZnO + Nitrogen (4%)	MWCNT (0.1 g) + Silver (3%) + ZnO + Nitrogen (4%)	MWCNT (0.1 g) + Silver (4%) + ZnO + Nitrogen (4%)
Sample Codes	P_1	P_2	P_3	P_4

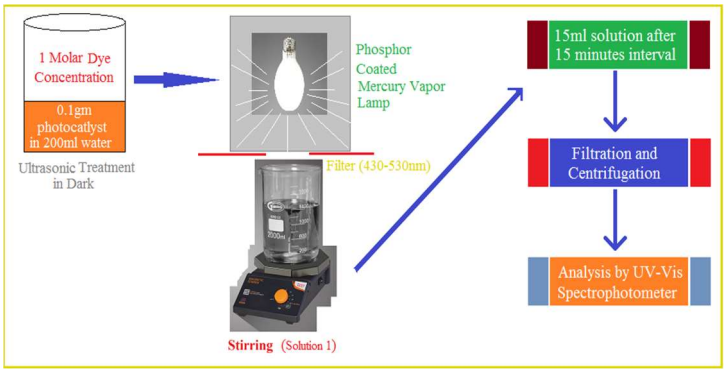

Fig.-3: The General Scheme of The Photocatalytic Degradation Of Dye

UV-visible and Photoluminescence Study

As the incident UV-Vis light consists of photons, the amount of absorbed photons provides the peak in the spectrophotometer. This peak varies with the amount the photons absorbed which is plotted against the wavelength. The corresponding peak provides detailed information regarding the specific wavelength of absorption, the concentration of solute, and the presence of impurities. Ultraviolet and visible (UV-vis) spectrophotometer was used for the measurement of absorption spectra of the synthesized nanocomposites. Fig.-5 (a), Absorption spectra of prepared samples show a red shift i.e., spectra shifted toward a higher wavelength with a rising in the percentage of dopants. UV-visible-NIR spectrophotometer (Perkin Elmer Lambda 20) was used for recording the absorption spectrum of samples in the range of 250–800 nm.[40]
ZnO is a direct band semiconductor [$(\alpha h\upsilon)^2$ Vs ($h\upsilon$), in Tauc's plot]. In Fig.-5 (b), the line obtained in Tuac's plot by extrapolating the x-axis provides the exact value of band gap energy (3.2, 2.75, 2.58, and 2.50 eV). In the case of photoluminescence analysis (Agilent Cary Eclipse), Absorption of light takes place after incidence on the sample by influencing its energy axis to the sample, and this phenomenon is known as photoexcitation.[41] Fig.-5 (c), oxygen antisemites, zinc vacancies, and oxygen interstitials are various defects that exist in the ZnO lattice shown by luminescence spectra. Intensity falls progressively with increasing doping percentage i.e., pure ZnO shows maximum intensity and maximum doped sample shows minimum

intensity can be correlated with progressive fall in charge carrier recombination speed with doping concentration.[42]

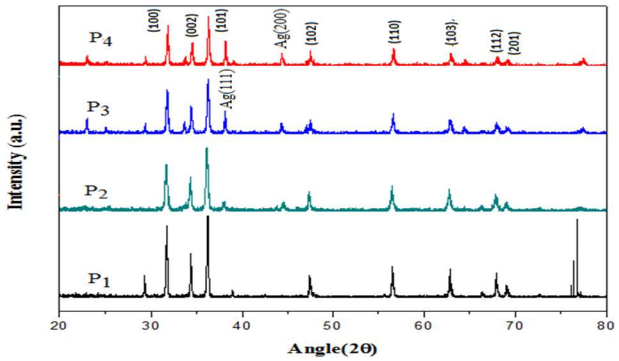

Fig.-4: X-Ray Diffraction Graph of the samples

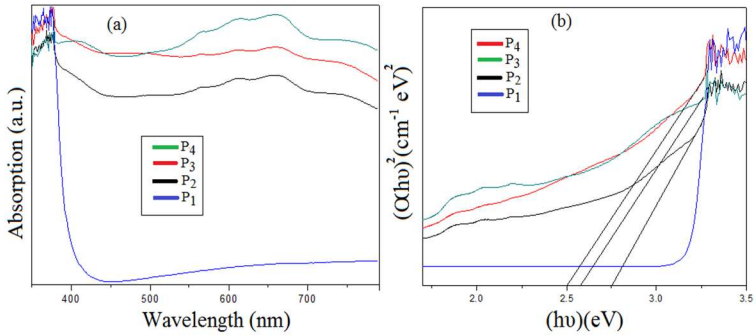

Fig.-5:(a) Absorption Spectra (b) Tauc's Plot of the Samples

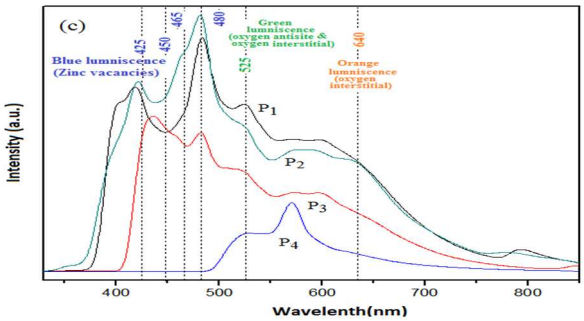

Fig.-5: (c) Photoluminescence Graph of the Samples

Morphological Study

Scanning electron microscope belongs to the class of electron microscopes, which is inured to determine the exterior morphology of the sample. This microscope scans the sample with a high-energy electron beam. In contrast, SEM (SU8010-HITACHI) uses an electron beam to magnify and visualize the sample.[43] In Fig.-6(a), shows the doped MWCNT/ZnO nanocomposite agglomerations with 19-34 nm diameters of CNT. EDX (Quantax 200) in combination with SEM shows Zn, O, Ag, and N elements in samples P_1 and P_4, in Fig.-6(b). In contrast to SEM, the electron beam used in the case of TEM (FEI-Technai G2 F20) is of higher energy which can penetrate through the ultrathin specimens,[44] TEM images of sample P_4 are shown in Fig.-6(c). The surface area of a solid material can be understood by the BET (Quantochrome) analysis. BET stands for a theory proposed by three scientists Brunauer–Emmett–Teller. It works on the phenomenon of physisorption or physical adsorption. In BET analysis of sample P_4, 115.7 m^2/gm of surface area, 2.2 nm pore diameter, and mesoporous morphology with type 4 hysteresis have been revealed. Type 4 hysteresis shapes refer to the ink bottle shape morphology of pores.[45]

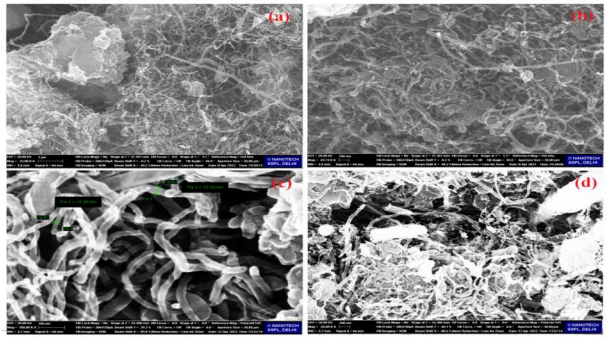

Fig.-6: (a) SEM Images of the Samples P_4 at Different Resolutions

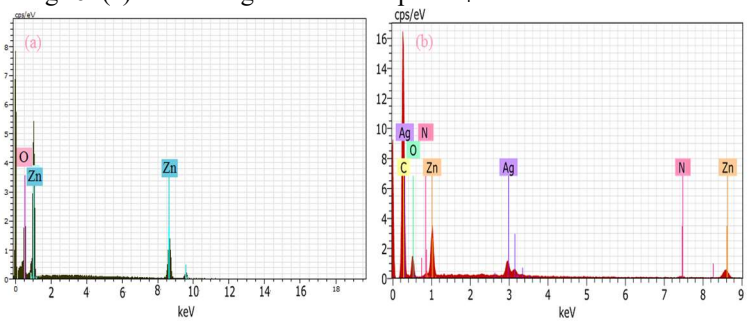

Fig.-6: (b) EDX Spectra of the Sample (a) P_1 and (b) P_4

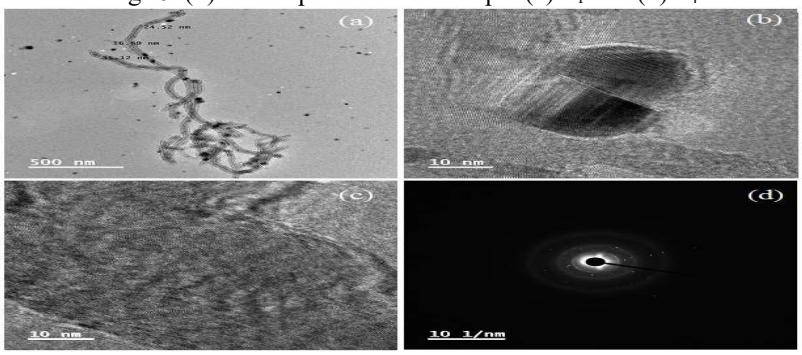

Fig.-6: (c) TEM Images of the Samples P_4 at Different Resolutions

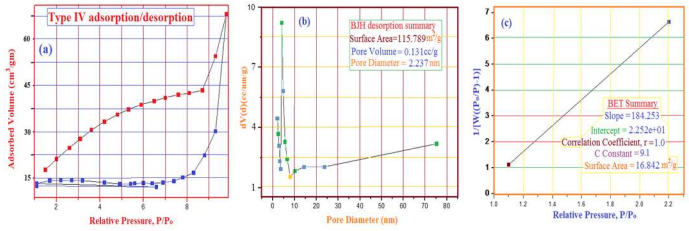

Fig.-7: (a) Adsorption-Desorption Graph (b) BJH desorption (c) BET Summary of the Samples P_4

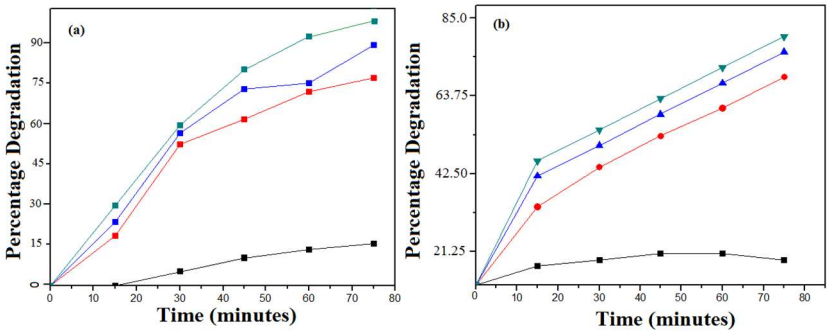

Fig.-8: Dye Degradation Pattern of (a) Methylene Blue (b) Congo Red

Table 2: Degradation Efficiencies of Photocatalyst After 90 Minutes

Sample	P_1	P_2	P_3	P_4
Congo Red	10%	65%	70%	80 %
Methylene Blue	14%	74%	87%	98 %

Photoexcitation of semiconductor nanoparticles leads to reduction and oxidation progression. Exposure of visible light source with the photocatalyst for the degradation of Congo red (497 nm, acidic dye) and Methylene blue (668 nm, basic dye) dyes in 90 minutes is shown in Fig.-3 and Fig.-8 (a-b). All the samples contained a fixed proportion of MWCNT and nitrogen and different proportion of silver. Prepared samples act as an efficient photocatalyst because of nanoscale size and crystalline nature as shown by TEM and XRD studies. With an increasing proportion of silver, the degradation of dyes increases due to a decrease in electron-hole recombination (Photoluminescence Study) and band gap energy (UV-vis study). Composite formation with carbon nanotubes is vital to provide an active site for adsorption, due to porous structure (BET study).

CONCLUSION

The photocatalytic performances towards the degradation of two dyes of all the samples were analyzed. In the subjection to visible radiance, the apical degeneracy was prosecuted in the content of P_4 (methylene blue (98%) and congo red (80%)). The hypothesis for the apical photocatalytic potential of porous ZnO nanocomposite was attributed to the task of the dopant to deprecate charge carrier activity, and reduction in the bandgap energy (as decided by UV-vis and PL spectroscopy). In the future, efforts can be made toward the integration of novel ZnO compounds based on advanced nanomaterials such as polymers, graphene, and metal-organic frameworks with synergistic photocatalytic properties. Further, the scope of this work can be extended toward the development of low-cost and commercially viable water treatment systems using sunlight as the source of energy.

ACKNOWLEDGMENTS

All the authors acknowledge and thank their respective institutes and universities of affiliation.

CONFLICT OF INTERESTS

The authors declare that there is no conflict of interest.

AUTHOR CONTRIBUTIONS

All the authors contributed significantly to this manuscript, participated in reviewing/editing, and approved the final draft for publication. The research profile of the authors can be verified from their ORCID ids, given below:

M. Singh https://orcid.org/0000-0003-3477-9641
P. Kumar https://orcid.org/0000-0002-8431-1062
N.S. Singh https://orcid.org/0000-0002-2783-1790
A. Jain https://orcid.org/0000-0003-4251-3915

REFERENCES

1. P.A. Shivajirao*, International Journal of Advanced Engineering Research and Studies,* (2012)
2. N. Chauhan, V. Singh, S. Kumar, M. Kumari and K. Sirohi, *Journal of Sol-Gel Science and Technology,* **90,** 390(2019), https://doi.org/10.1007/s10971-019-04969-6
3. N. Tripathy, R. Ahmad, H. Kuk, Y.B. Hahn and G. Khang, *Ceramics International*, **42(8)**, 9519(2016), https://doi.org/10.1016/j.ceramint.2016.03.030
4. M.I. Khan, *Results in Physics*, **7**, 3176(2017), https://doi.org/10.1016/j.rinp.2017.08.038
5. H- Y. He, *Micro and Nanosystems*, **6(2)**, 103(2014), http://dx.doi.org/10.2174/1876402906666140912005237
6. P. Bhardwaj, S. Kaushik, P. Gairola and S.P. Gairola, *Journal of Polymer Engineering*, **39(3)**, 228(2019), https://doi.org/10.1515/polyeng-2018-0292
7. P. Bhardwaj and A.N. Grace, *Diamond and Related Materials*, **106**, 107871(2020), https://doi.org/10.1016/j.diamond.2020.107871

8. A.K. Sharma, P. Bhardwaj, S. Kumar and D.Y. Sharma, *Advanced Materials Letters*, **6(5)**, 414(2015), https://dx.doi.org/10.5185/amlett.2015.5690
9. A.K. Sharma, G. Chaudhary, P. Bhardwaj, I. Kaushal and S. Duhan, *Current Analytical Chemistry*, **13(4)**, 277(2017), http://dx.doi.org/10.2174/1573411012666160624080450
10. P. Bhardwaj, S. Kaushik, P. Gairola and S. P. Gairola, *SN Applied Sciences*, **1**, 113(2019), https://doi.org/10.1007/s42452-018-0115-7
11. P. Bhardwaj, S. Kaushik, P. Gairola and S.P. Gairola, *Radiation Physics and Chemistry*, **151**, 156(2018), https://doi.org/10.1016/j.radphyschem.2018.06.001
12. A.K. Sharma, P. Bhardwaj, K.K. Singh and S.K. Dhawan, *Applied Nanoscience*, **5**, 635(2015), https://doi.org/10.1007/s13204-014-0362-x
13. G. Chaudhary, A.K. Sharma, P. Bhardwaj, K. Kant, I. Kaushal and A.K. Mishra, *Journal of Energy Chemistry*, **26(1)**, 175(2017), https://doi.org/10.1016/j.jechem.2016.09.013
14. K. M. Sreedhar, S. Sivan, K. Raja, K. Suresh, R. Sreelekshmi, A. Palat and K. M. Sreekanth, *Rasayan Journal of Chemistry,* **14(2)**, 1289(2021), http://dx.doi.org/10.31788/ RJC.2021.1426031
15. V. Prasad, G.G. Simiyon, A.E. Mammen and N. Jayaprakash, *Rasayan Journal of Chemistry,* **12(2)**, 860(2019), http://dx.doi.org/10.31788/RJC.2019.1225226
16. A. Raj and R. Lawerence, *Rasayan Journal of Chemistry,* **11(3)**, 1339(2018), http://dx.doi.org/10.31788/RJC.2018.1132009
17. P.P. Thattil and A.L. Rose, *Rasayan Journal of Chemistry,* **13(2)**, 1166(2020), http://dx.doi.org/10.31788/RJC.2020.1325558
18. M. Dagar, S. Kumar, A. Jain, A. Vohra and P. Kumar, *Journal of the Australian Ceramic Society*, **58**, 1571(2022), https://doi.org/10.1007/s41779-022-00795-2
19. R. Nivetha, K. Gothandapani, V. Raghavan et al., *ACS Omega*, **5(30)**, 18941(2020), https://doi.org/10.1021/acsomega.0c02171
20. R. Nivetha et al., *Materials Research Express*, **7,** 114001(2020), https://doi.org/10.1088/2053-1591/abb056
21. N. Chauhan, V. Singh, S. Kumar, K. Sirohi and S. Siwatch, *Journal of Sol-gel Science Technology*, **91**, 567(2019), https://doi.org/10.1007/s10971-019-05059-3
22. A.T.A. Saleh, M.A. Gondal, Q.A. Drmosh, Z.H. Yamani and A. AL-yamani, *Chemical Engineering Journal*, **166(1)**, 407(2011), https://doi.org/10.1016/j.cej.2010.10.070
23. M. Ahmad, E. Ahmed, Z.L. Hong, W. Ahmed, A. Elhissi and N.R. Khalid, *Ultrasonics Sonochemistry*, **21(2)**, 761(2014), https://doi.org/10.1016/j.ultsonch.2013.08.014
24. P. Liu, Y. Guo, Q. Xu, F. Wang, Y. Li and K. Shao, *Ceramics International*, **40(4)**, 5629(2014), https://doi.org/10.1016/j.ceramint.2013.10.157
25. I.Y.Y. Bu, *Materials Science in Semiconductor Processing*, **22**, 76(2014), https://doi.org/10.1016/j.mssp.2014.01.043
26. M. Elias, S. Akter, M.A. Hossain and M.H. Suhag, *Thin Solid Films*, **717**, 138472(2021), https://doi.org/10.1016/j.tsf.2020.138472
27. S.D. Dalt, A.K. Alves and C.P. Bergmann, *Materials Research*, **19(6)**, 1372(2016), http://dx.doi.org/10.1590/1980-5373-mr-2016-0036
28. M.M. Reddy, G.R. Reddy, K. Chennakesavulu et al., *Journal of Porous Materials*, **24**, 149(2017), https://doi.org/10.1007/s10934-016-0247-3
29. X. WANG, S. YAO and X. LI, *Chinese Journal of Chemistry*, **27**, 1317(2009), https://doi.org/10.1002/cjoc.200990220
30. T.A. Saleh et al., *Nanotechnology*, **21(49)**, 495705(2010), http://dx.doi.org/10.1088/0957-4484/21/49/495705
31. M. Elias, M.N. Uddin, J.K. Saha et al., *Molecules*, **26(5)**, 1470(2021), https://doi.org/10.3390/molecules26051470
32. S. Okeil, J. Krausmann, I. Dönges, S. Pfleger, J. Engstlera and J.J. Schneider, *Dalton Transactions*, **46**, 5189(2017), https://doi.org/10.1039/C7DT00407A
33. M.H.A. Azqhandi, B. Vasheghani F, F.H. Rajabi and M. Keramati, *Results in Physics*, **7**, 1106(2017), https://doi.org/10.1016/j.rinp.2017.02.033

34. N. Chauhan, V. Singh, S. Kumar and A. Vohra, *Arabian Journal for Science and Engineering*, **47**, 6989(2022), https://doi.org/10.1007/s13369-021-06280-5
35. M. Basit, M. Abbas, N. Ahmad, S. Javed and N.A. Shah, *Frontiers in Materials*, **9**(2022), https://doi.org/10.3389/fmats.2022.835521
36. L.M. Cursaru, S.N. Valsan, M.E. Puscasu et al., *Materials (Basel)*, **14(18),** 5330(2021), https://doi.org/10.3390/ma14185330
37. M. Escobar, M.S. Moreno, R.J. Candal et al., *Applied Surface Science*, **254(1)**, 251(2007), https://doi.org/10.1016/j.apsusc.2007.07.044
38. N. Chauhan, V. Singh, S. Kumar and R. L. Dhiman, *Arabian Journal of Science and Engineering*, **45,** 249(2020), https://doi.org/10.1007/s13369-019-04291-x
39. P. Bindu and S. Thomas, *Journal of Theoretical and Applied Physics*, **8**, 123(2014), https://doi.org/10.1007/s40094-014-0141-9
40. A.M. Putz, A. Len, C. Ianăşi, C. Savii and L. Almásy, *Korean Journal of Chemical Engineering*, **33**, 749(2016), https://doi.org/10.1007/s11814-016-0021-x
41. E.G. Goh, X. Xu and P.G. McCormick, *Scripta Materialia*, **78-79**, 49(2014), https://doi.org/10.1016/j.scriptamat.2014.01.033
42. I. Kazeminezhad, S. Saadatmand and R. Yousefi, *Bulletin of Materials Science*, **39**, 719(2016), https://doi.org/10.1007/s12034-016-1206-y
43. A. Katiyar, N. Kumar and A. Srivastava, *Materials Today: Proceedings*, **5**, 9144(2018), https://doi.org/10.1016/j.matpr.2017.10.034
44. M. Manzoor, A. Rafiq, M. Ikram, M. Nafees and S. Ali, *International Nano Letters*, **8**, 1(2018), https://doi.org/10.1007/s40089-018-0225-7
45. Pankaj Attri, Yong Hee Kim, Dae Hoon Park, Ji Hoon Park, Young J. Hong, Han Sup Uhm, Kyoung-Nam Kim, Alexander Fridman and Eun Ha Choi, *Scientific Reports*, **5**, 9332 (2015), https://doi.org/10.1038/srep09332

[RJC-8076/2022]